STRUCTURAL, OPTICAL, AND VISIBLE-LIGHT DRIVEN PHOTACATALYTIC PROPERTIES OF Yb-DOPED $BiVO_4$ NANOPARTICLES PREPARED VIA RAPID SONOCHEMICAL PROCESS

Kanokthip Boonyarattanakalin, Tanisara Noinonmueng, Thanaphon Kansaard, Tirapat Wechprasit, Wanichaya Mekprasart, Kanoknan Phacheerak, Wisanu Pecharapa*, and Anuchit Jaruvanawat

Received: January 08, 2022; Revised: July 22, 2022; Accepted: July 25, 2022

Abstract

This work represents the synthesis and structural, morphological, and optical characterization of rare-earth Yb-doped $BiVO_4$ materials with different Ytterbium (Yb^{3+}) contents (0% - 5%). Yb-doped $BiVO_4$ specimens in form of fine nanoparticles were synthesized by a rapid and facile sonochemical process. The structural and morphological characterizations were observed by X-ray diffraction technique (XRD), Fourier transform infrared spectroscopy (FTIR), and scanning electron microscopy (SEM). Important optical properties of the prepared samples were investigated by the diffuse reflectance technique and the corresponding optical band gaps were calculated by the mean of the Kullbelka-Munk equation. From the characterized results, it is acknowledged that incorporated Yb dopant has a significant effect on the crystalline structure of $BiVO_4$ by reducing in monoclinic phase in the pristine sample while the increasing Yb doping composition resulted in the mixed phases of monoclinic and tetragonal phases since Yb^{3+} ions could probably induce the stabilization of the tetragonal phase in $BiVO_4$ material. Moreover, extensive doping with Yb^{3+} exhibits considerable influence on not only structural but also optical and relevant visible - driven photocatalytic properties of $BiVO_4$ by means of the color degradation of RhB dye solution.

Keywords: **Bismuth vanadate, Ytterbium, Photocatalyst, Sonochemical process**

Introduction

Up to now, the industrial expansion has significantly caused serious environmental problems including air pollution, soil pollution, and water pollution, especially water pollution drained out from industrial factories as wastewater into the environment. This problem is becoming more severe and greatly concerned day by day (Bohn *et at*., 2008; Mekonnen *et al*., 2016; Oki *et al*., 2016). Therefore, the technology development for wastewater treatment especially by photocatalytic material is widely of interest. Among practical photocatalysts, Bismuth Vanadate ($BiVO_4$) is one of the promising semiconductive photocatalyst materials that can be activated by visible light irradiation. The Bismuth Vanadate is an outstanding semiconductor with a great photocatalytic capability to remove organic contaminants in wastewater (Ahmed *et al*., 2017; Dolic´ *et al*., 2018), especially with the improvement in its performance by doping with rare earth elements (Xu *et al.,* 2009) leading to considerable enhancement in dye removal mechanism. Recently, much literature stated that

College of Materials Innovation and Technology, King Mongkut's Institute of Technology Ladkrabang, Ladkrabang / Bangkok, 10520, Thailand. E-mail: wisanu.pe@kmitl.ac.th
* *Corresponding author*

rare-earth elements such as Nd^{3+} (Tan *et al.*, 2015a), Sm^{3+} (Tan *et al.*, 2015b), and Gd^{3+} (Lao *et al.*, 2015) are considered as co-catalysts and active addition that noticeably increases photocatalytic efficiency of Bismuth Vanadate matrix. A further report by Tan *et al.*, 2014 (Tan *et al.*, 2014) explained that the incorporation of Yb^{3+} ions with certain content in Bismuth Vanadate can ameliorate the photocatalytic functionality of Bismuth Vanadate. It has been reported that the stability of the tetragonal phase and enhanced photocatalytic performance of $BiVO_4$ can be achieved by substituting Bi^{3+} sites with lanthanide ions that have a close ionic radius to Bi^{3+} (117 pm) (San *et al*., 2021). Yb^{3+} ion whose ionic radius of 101 pm could be considered to be a potential dopant to well substitute at Bi^{3+}, resulting in the expectation of stabilized tetragonal $BiVO_4$ with good photocatalytic activity.

This research reports the preparation process of $BiVO_4$ and Yb-doped $BiVO_4$ nanoparticles via a rapid sonochemical process without post-treatment requirements. Relevant structural and optical properties of the prepared samples were extensively characterized by XRD, FTIR, SEM, and DRS techniques. The photocatalytic activity was evaluated by degradation of Rhodamine B organic dye using as a model of organic compound in an aqueous solution under visible light irradiation generated by Xe-Lamp (300W).

Materials and Methods

Synthesis of Yb-doped $BiVO_4$ powder

For the sonochemical synthesis of Yb-doped $BiVO_4$, 0.01mol of bismuth nitrate pentahydrate ($Bi(NO_3)•5H_2O$) and 0.01 mol of ammonium metavanadate (NH_4VO_3) were designated as starting source of Bi and V was separately dissolved in 100 ml deionized water (DI-water). After that, different contents of Ytterbium nitrate ($Yb(NO_3)_3)•6H_2O$) with the molar ratio of Yb and Bi from 0 at% to 5 at% were dissolved in 10 ml DI water. After mixing the three solutions, a certain amount of ammonia (NH_3) solution was added dropwise into the mixed solution for pH adjustment to reach pH=7 then kept continued stirring for 5 min at room temperature until a yellowish aqueous solution was obtained. The mixed precursor solution containing Bi, V, and different Yb doping concentrations was poured into the sonochemical chamber then the operation was conducted under ultrahigh ultrasonic (20kHz) irradiation with a power of 750W for 30 min. Finally, the precipitated products were separated, washed with DI water, and dried in an oven at 100°C for 24 h to obtain as-prepared samples.

Characterizations

The crystallinity and morphology of all specimens were investigated by X-ray diffraction (Rigaku Smart Lab) and FE-SEM techniques, respectively. The type of chemical bonding and functional groups of as-prepared samples was characterized by Fourier transform infrared spectrometer (PerkinElmer Scientific, spectrum Two) while the optical property of all samples was characterized by Diffuse reflectance spectrophotometer (HITACHI, UH4150) and the corresponding optical band gap (E_g) was evaluated by using Kubelka-Munk calculation.

Photocatalytic performance

The photocatalytic performance of the bared $BiVO_4$ and Yb-doped $BiVO_4$ samples was determined by photodecomposition of organic dye by using Rhodamine B (RhB) as an organic compound model operated under visible light illumination generated by Xe-lamp (300Watts). Firstly, 0.01 M of RhB solution and 0.1 g of photocatalyst sample was mixed and continuously stirred in a dark place for 30 minutes to confirm the absorption/desorption of photocatalyst specimen, and 5 ml of the mixed solution was chosen for determination of RhB concentration by photoabsorption with UV-visible spectrophotometer (A_0). After that, the Xe-lamp was switched on until the solution became a clear solution for activity achievement. Every 5 min on the turned-on Xe-lamp, the solution sample was extracted for concentration evaluation (A_t). The photodecomposition rate (k) can be calculated by the following equation, $A_t = A_0 \exp(-kt)$.

Results and Discussion

Figure 1 shows the XRD patterns of pure $BiVO_4$ and Yb-doped $BiVO_4$. Pure $BiVO_4$ (0at.%) exhibits prominent main diffraction peaks located at 28.9° and 30.5° corresponding to the orientation planes (112), (004) of $BiVO_4$ with monoclinic phase (JCPDS no. 01-083-1699) without any secondary traces of Bi- and V-related oxides or impurities. This result suggests that pure monoclinic $BiVO_4$ powder can be synthesized by a one-step sonochemical process. Furthermore, as observed in the doped samples, the characteristic peaks of monoclinic $BiVO_4$ obviously decrease but the appearance of the tetragonal phase tends to increase as Yb doping content is 1%. Beyond this doping content, the corresponding XRD patterns exhibit a complete tetragonal phase with associated peaks situated at 24.5° for (200) plane and 32.7° for (112) plane

(JCPDS no.00-014-0133). This feature implies that phase transformation from monoclinic to the tetragonal structure of $BiVO_4$ is strongly influenced by the incorporation of Yb which is in harmony with the previous research work reported by S. Obregón and G. Colón (Colón *et al.*, 2014). This change in the structural phase induced by Yb could be explained by the Yb^{3+} substitution at Bi^{3+}site in the $BiVO_4$ structure. Naturally, Ytterbium (Yb^{3+}) ions with a smaller ionic radius (101 pm with 6 coordination number) would prefer to occupy the Bi^{3+} position with a greater ionic radius (117 pm with 6 coordination number) (Shannon, 1976) resulting in the favorable tetragonal phase crystallization of the doped samples. To further investigate the effect of Yb doping content on the crystallinity of $BiVO_4$, the tetragonal: monoclinic ratio extracted from XRD patterns was calculated by using the intensity of the main peaks at 24.5° and 28.9° for tetragonal and monoclinic phases, respectively. The values of the tetragonal: monoclinic ratio with different Yb doping contents are reported in Table 1. It is indicated that the ratio increases drastically to 15 as the matrix is incorporated with only 2% of Yb dopant and can reach the maximum value of 18 as the doping content is 4%. This result confirms the preference and stability of the tetragonal phase can be achieved by increasing the Yb dopant.

The average crystal size of each sample was calculated from the full width at half maximum (FWHM) of (112) peak for the monoclinic phase and (101) peak for the tetragonal phase using Scherrer's equation expressed by Equation (1).

$$D = \frac{K\lambda}{\beta \cos\theta} \quad (1)$$

Note that, D is the calculated crystallite size of the sample, constant K (0.9) is the shape factor, λ is the wavelength of Cu K_α (1.54 Å), β is the full-width at half maximum (FWHM) collected by the deconvolution of the raw XRD data and θ is the diffracted angle. The calculated average crystallite sizes of undoped and doped $BiVO_4$ are listed in Table 1. It is observed that the average crystallite size of Yb-doped $BiVO_4$ tends to shrink with increasing Yb dopant. This significant change in crystallite size is probably due to microscopic strain induced by the difference in ionic radii of Bi^{3+} and Yb^{3+} that is preferable to substitute at the Bi site. This induced strain could consequently affect the lattice distortion and deterioration in host $BiVO_4$ crystal growth. In addition, the significant change in crystallite size with increasing dopant could be associated with the phase change from monoclinic to tetragonal structure with different unit cell volume, resulting in considerable shrinkage in its crystallite size. Phase change and diminished crystallite size in $BiVO_4$ that are highly influenced by Yb^{3+} dopant are in accordance with the decrease and broadening in XRD peaks. (Huang *et al.*, 2014).

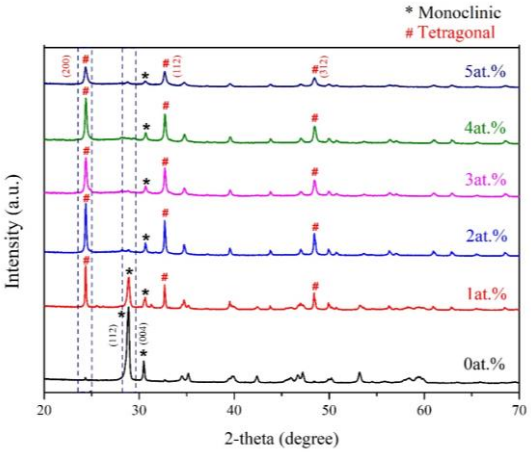

Figure 1. XRD patterns of Yb-doped $BiVO_4$ powders with different doping contents

Table 1. Major crystal structure and band gap energy of pure $BiVO_4$ and Yb-doped $BiVO_4$ with different doping contents

Samples	Crystal structure	tetragonal: monoclinic ratio	Average crystallite size (nm)	band gap energy (eV)
Undoped	Monoclinic	0.02	21.56	2.59
1 at.% Yb^{3+}	Monoclinic/ Tetragonal	1.38	17.03	2.60
2 at.% Yb^{3+}	Tetragonal	15.02	21.97	3.01
3 at.% Yb^{3+}	Tetragonal	10.61	16.97	3.03
4 at.% Yb^{3+}	Tetragonal	18.41	16.99	3.04
5 at.% Yb^{3+}	Tetragonal	14.09	16.33	3.04

The morphologies of the $BiVO_4$ samples synthesized by the sonochemical process were characterized by FE-SEM, as shown in Figure 2. For bare $BiVO_4$ the particle possesses irregular flake-like morphology with ~200 nm thick (Figure 2(a)). As the doping content increases, the morphologies of the products are not different, but their average crystal size noticeably tends to decrease with increasing doping content which could be related to the monoclinic-to-tetragonal phase transformation of the product.

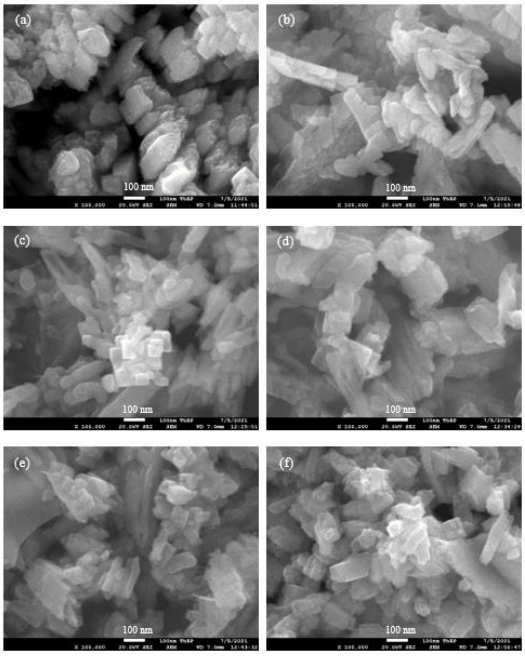

Figure 2. FE-SEM images of (a) pure $BiVO_4$ and $BiVO_4$ doped with Yb content of (b) 1 at.% (c) 2 at.% (d) 3 at.% (e) 4 at.% (f) 5 at.%

Fourier transform infrared spectroscopy (FTIR) recorded in the range of 400-2000 cm^{-1} was used to verify the chemical bonding of the synthesized Yb-doped $BiVO_4$ prepared with different contents of Yb^{3+}. Figure 3. shows the absorption band at 700-900 cm^{-1} with the peak position at 720 cm^{-1} assigned to the asymmetric stretching and symmetric stretching vibration of the V-O bonds (Sivakumar *et al.*, 2015). The characteristic band peak at 608 cm^{-1} observed in the undoped sample is ascribed to the symmetric stretching vibration mode of V-O-V units that are found to be disappeared in the doped samples that would be related to the phase transformation as revealed by XRD results. Meanwhile, the observable band at around 1042 cm^{-1} could be associated with the unshared V=O stretching mode. The broad band in the range of 1,300-1,450 cm^{-1}could be ascribed to c-related residue or atmospheric absorbed carbon dioxide (Wang *et al.*, 2017).

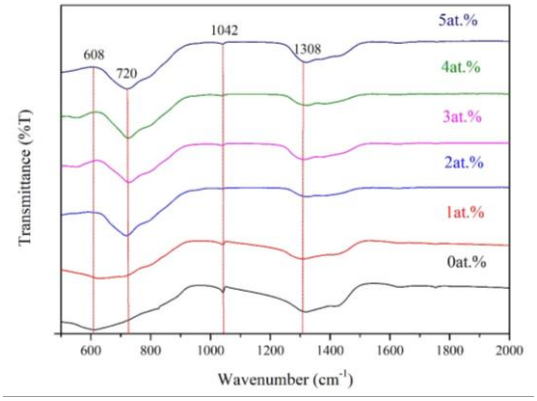

Figure 3. FTIR spectra of pure $BiVO_4$ and Yb-doped $BiVO_4$ with different doping contents

Figure 4. illustrates the resulting UV-VIS diffuse reflectance spectra (DRS) of pure $BiVO_4$ and Yb-doped $BiVO_4$. The pure $BiVO_4$ sample shows high optical reflection for the wavelength greater than 453 nm while the Yb-doped $BiVO_4$ samples clearly exhibit high reflection for the shorter wavelength at around 385 nm. This significant difference in the edge of the reflection wavelength is associated with the characteristic optical band gap of the monoclinic phase for undoped $BiVO_4$ and the tetragonal phase for doped samples. Further evaluation of corresponding optical band gap energy (E_g) extracted from DRS results was carried out using Kubelka-Munk calculation (Kansaard *et al.*, 2021) The calculated value along with the major phase of the prepared samples are summarized in Table 1. It is found that the optical band gap of pure $BiVO_4$ with monoclinic phase is approximately 2.59 eV and Yb-doped $BiVO_4$ with tetragonal major phase is around 3.04 eV, respectively. The increase of E_g in Yb-doped $BiVO_4$ samples is originated from the $BiVO_4$ phase transition from monoclinic to tetragonal phase relating to the change of electronic structure as strong absorption in the UV region with Yb-doped $BiVO_4$ sample (Huang *et al.*, 2014).

Photocatalytic activity of pure $BiVO_4$ and Yb-doped $BiVO_4$ were evaluated by degradation RhB under visible light irradiation and corresponding results are shown in Figure 5. It is clearly observed that the decomposition efficiency of RhB greatly increases with increasing Yb loading content in $BiVO_4$. Effectively complete decomposition of the RhB can be realized within 30 min under visible light.

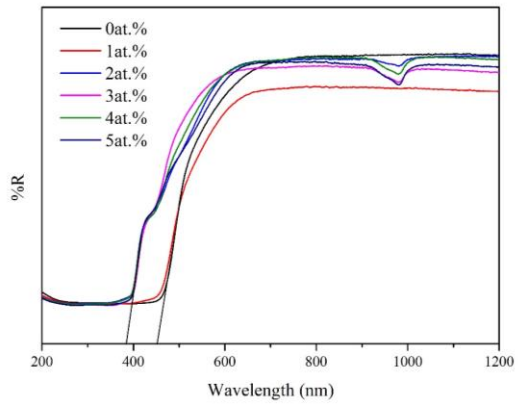

Figure 4. Diffuse reflectance spectra of pure $BiVO_4$ and Yb-doped $BiVO_4$ with different doping contents

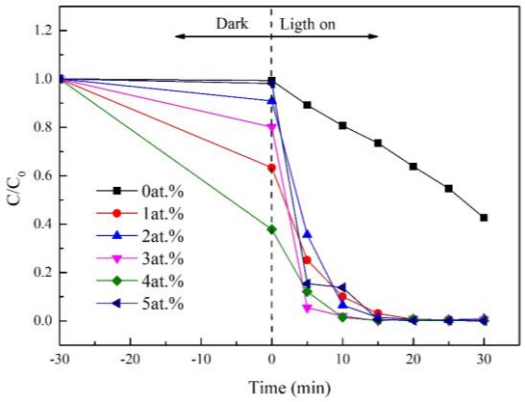

Figure 5. Photocatalytic degradation of RhB by Yb-doped $BiVO_4$ with different doping contents

Two mechanisms of adsorption of RhB on the catalyst surface and photogenerated electron-hole pairs under the illumination of the photocatalyst are responsible for the functionally photocatalytic activity of $BiVO_4$. Typically, under illumination, photons with greater energy than the band gap energy of $BiVO_4$ can excite the electrons from its valence band to its conduction band (CB), leaving unpaired holes at the valence band (VB). Excited electrons at CB can react with O_2 at the surface to form a superoxide anion radical ($O_2^{\bullet-}$). This $O_2^{\bullet-}$ radical is an efficient oxidizing agent to degrade the dye molecule into non-toxic organic compounds (Sivakumar *et al.*, 2015). The degradation of RhB for Yb-doped $BiVO_4$ content (1-5at. %) can reach more than 99% after 30 min under visible light, while that of pure $BiVO_4$ is just only 57%. The superiority in photocatalytic performance is attained for 5 at.% Yb-doped $BiVO_4$ as it can reach 99.95% within 30 min. This enhancement in photocatalytic performance when doping with Yb could result from the fact that the incorporated Yb could induce the creation of the trap state aligning between the conduction and valence band of $BiVO_4$. This state could retard the recombination of photo-generated electron-hole pairs resulting in considerable enhancement in the doped samples (Bang *et al.*, 2020).

Conclusions

In this work, Yb-doped $BiVO_4$ powder prepared by a one-step sonochemical process is reported. The effect of Yb^{3+} doping contents (0-5at.%) on the phase transformation from monoclinic to tetragonal phase is evaluated by XRD and FTIR results. FE-SEM images show the irregular flake-like shape of the prepared samples with decreasing size as the doping content increases. Optical properties and corresponding band gaps were investigated by DRS result and it is found that the change in optical properties is correlated to the phase transformation induced by the Yb dopant. The photocatalytic performance of the prepared specimen through RhB dye degradation under visible light is enhanced by the incorporation of Yb which could be due to the retardment of electron-hole recombination by the trap state induced by Yb dopant. The superior photocatalytic performance is attained for 5at.% Yb-doped $BiVO_4$ with a value of 99.95% within 30 minutes.

Acknowledgement

This research grant has been supported by King Mongkut's Institute of Technology Ladkrabang (Grant No. RE-KRIS/021/64). The authors would like to thank College of Materials Innovation and Technology, King Mongkut's Institute of Technology Ladkrabang (KMITL) for supporting characterization facilities.

References

Ahmed, T., Zhang, K.L., Gao, Y.Y., Xu, H.B., and Zhang, Y. (2017). Surfactant-free synthesis of m-$BiVO_4$ nanoribbons and enhanced visible-light photocatalytic properties. Materials Research Bulletin, 99:298-305.

Bang, H.J., Lee, H., Park, Y.K., Kim, H., Ha, H.H., Yu, Y.H., Kim, S.J., and Jung, S.C. (2020). Fabrication of Yb-doped TiO_2 using liquid phase plasma process and its photocatalytic degradation activity of naproxen. Journal of Materials Science., 55:9,665-9,675.

Bohn, P.W., Elimelech, M., Shannon, M.A., Georgiadis, T.G., Mariñas, B.J., and Mayes, A.M. (2008). Science and technology for water purification in the coming decades. Nature Reviews, 425:301-310.

Colón, G. and Obrego´n, S. (2014). Excellent photocatalytic activity of Yb^{3+}, Er^{3+} co-doped $BiVO_4$ photocatalyst. Applied Catalysis B: Environmental, 152(153):328-334.

Dolic´, D.S., Jovanovic´, D.J., Smits, K., Marinovic´-Cincovic´, M., Polobic´, S., and Dramicanin, M.D. (2018). A comparative study of photocatalytically active nanocrystalline tetragonal zircon-type and monoclinic scheelite-type bismuth vanadate. Ceramic International., 44(15):17,953-17,961.

Huang, J., Tan, G., Zhang, L., Ren, H., Xia, A., and Zhao, C. (2014). Enhanced photocatalytic activity of tetragonal $BiVO_4$: Influenced by rare earth ion Yb^{3+}. Materials Letters., 133:20-23.

Kansaard, T., Bangbai, C., Jayasankar, C.K., and Pecharapa, W. (2021). Effect of ultrasonic irradiation time on physical properties and photocatalytic performance $BiVO_4$ nanoparticles prepared via sonochemical process. Integrated Ferroelectrics, 214:123-132.

Lao, Y., Tan, Guoqiang., Dong, G., Ren, H., and Xia, A. (2015). A comprehensive investigation of tetragonal Gd-doped $BiVO_4$ with enhanced photocatalytic performance under sunlight. Applied Surface Science., 364:156-165.

Mekonnen, M.M. and Hoekstra, A. (2016). Four billion people facing severe water scarcity. Science Advances, 2:e1500323.

Oki, T. and Kanae, S. (2016). Global Hydrological Cycles And World Water Resources. Science., 313(5,790):1,068-1,072.

Sivakumar, V., Suresh, R., Giribabu, K., and Narayanan, V. (2015) $BiVO_4$ nanoparticles: Preparation, characterization and photocatalytic activity. Cogent Chemistry, 1:1,074,647

Shannon, R.D. (1976). Revised effective ionic radii and systematic studies of interatomic distances in halides and chalcogenides. Acta Crystallographica Section A., 32(5):751-767.

San, J., Zhang, Z., Suo, H., Chen, Y., Xiang, J., and Guo, Ch. (2021). Temperature self-monitoring photothermal nano-particles of Er^{3+}/Yb^{3+} Co-doped zircon-tetragonal $BiVO_4$. Ceramics International, 47:409-415.

Tan, G., Luo, Y., Dong. G., and Xia, A. (2015a). Effects of structure, morphology, and up-conversion on Nd-doped $BiVO_4$ system with high photocatalytic activity. Ceramic International., 41(2):3,259-3,268.

Tan, G., Luo, Y., Dong. G., Zhang, L., Hung, J., and Yang, W. (2015b). Structural transition of Sm^{3+} doped $BiVO_4$ with high photocatalytic activity under simulated sun-light. Applied Surface Science., 324:505-511.

Tan, G., Huang, J., Zhang, L., Ren, H., Xia, A., and Zhao, C. (2014). Enhanced photocatalytic activity of tetragonal $BiVO_4$: Influenced by rare earth ion Yb^{3+}. Material Letters, 133:20-23.

Wang, M., Zhang, Z., Cui, W., and Sui, H. (2017) Synthesis And characterization of a core-shell $BiVO_4$@g-C_3N_4 photo-catalyst with enhanced photocatalytic activity under visible light irradiation. RSC Advances, 7:8,167-8,177.

Xu, H., Wu, C., Li, H., Chu, J., Sun, G., Xu, Y. and Yan, Y. (2009). Synthesis, characterization and photocatalytic activities of rare earth-loaded BiVO4 catalysts. Applied Surface Science. 256(3):597-602.